JOURNAL OF MATERIALS SCIENCE 31 (1996) 5059–5067

Phase equilibria of the ternary Ag–Cu–Ni system and the interfacial reactions in the Ag–Cu/Ni couples

HUEY-TSYR LUO, SINN-WEN CHEN
Department of Chemical Engineering, National Tsing-Hua University, Hsin-Chu, Taiwan 30043, ROC

The phases formed at the interfaces of nickel and Ag–Cu alloys were determined by studying the reaction diffusion couples together with the isothermal sections of the Ag–Cu–Ni system at the annealing temperatures. Phase equilibria at 860, 795 and 700 °C, were determined by both experimental investigation and model calculation. The reaction diffusion couples were prepared with either the Ag–15 wt % Cu alloy with nickel foil, or Ag–28 wt % Cu alloy with nickel foil, and were annealed at the three above-mentioned temperatures. The interfaces of the reaction layers in the couples were non-planar. By using microscopes and EPMA, the phase sequences formed in the reaction diffusion couples were determined. These diffusion paths were in agreement with the phase equilibria study, and it demonstrated that the tie triangle shifted towards the nickel side as temperature increased. The thickness of the reacted layers was determined by using an image analyser, and a parabolic growth was found for the Ni/Ag–28 wt % Cu couple annealed at 795 °C.

1. Introduction

Ceramics have been intensively used in the advancing electronic packaging applications owing to their high thermal conductivity, better dielectric constant, closer thermal expansion coefficient to that of silicon chips, and most important, the ability of hermetic packaging [1–3]. The Ag–Cu–Ni system is of importance to the growing industry of ceramic packaging [3–5]; the Ag–Cu alloys are the most commonly used brazes in the ceramic packaging. Nickel pads are usually plated on the ceramic substrates to improve the brazability between the ceramic and the metals. The molten Ag–Cu braze reacts with the solid nickel and thus chemical bonding is formed at the interface during the brazing process.

The interfacial reactions are crucial for the strength of the joint and the reliability of the electronic products. Studies of the interfacial reactions are very intensive [5–18]; however, most of the studies concern only the reactions between solids and solid substrates [6–12]. Investigations regarding the molten solders' reaction with solid substrates are very limited, and are even more scarce for the reactions between molten brazes with solid substrates [5, 13–18]. The duration of the joining process is short; nevertheless, the rate of interfacial reaction between the molten braze (or solder) with the solid substrate, which occurs during the joining process, is much faster than that between the solid braze (or solder) with the solid substrate. Even during such a short period of the joining-processing time, a rather significant interfacial reaction has already occurred. The reaction layers formed during the joining process have direct impact upon the properties of the electronic products, and also have profound effects upon the phase formations at the interfaces of the products in subsequent usage under the solid/solid condition.

The present investigation was undertaken to study the reactions between the molten Ag–Cu alloys and the solid nickel substrate in detail. The interfacial reactions are driven by the nature of the phase equilibria and are constrained by kinetics; therefore, a fundamental understanding of the Ag–Cu–Ni phase equilibria is essential. In this study, both experimental and theoretical investigations have been carried out to assess the phase equilibria of the Ag–Cu–Ni systems. Owing to the tiny sizes of the nickel pad and the Ag–Cu braze, it is very difficult to quantify the interfacial reactions in the standard electronic packaging. Quantitative investigations of the interfacial reactions have been conducted by using the Ni/Ag–Cu reaction diffusion couples.

2. Experimental procedure

2.1. Alloy preparation

Two different binary Ag–Cu alloys were prepared for the diffusion couple study. The nominal compositions were Ag–28 wt % Cu and Ag–15 wt % Cu, and were prepared by using 99.99% pure silver and 99.999% pure copper shots. Silver and copper were weighed to an accuracy of $\pm$ 0.001 g, and melted in a vacuum furnace at 1100 °C under a 10^{-3} torr (1 torr = 133.322 Pa) vacuum for 2 h. The alloy was then removed from

0022–2461

the furnace, and sealed in a quartz tube under a 10^{-3} torr vacuum. The sample capsule was held in a tube furnace at 950 °C for 4 h, and then quenched into icy water. 60 mg alloy was sampled from the quenched alloy ingot for the examination of compositional homogeneity by using inductively coupled plasma (ICP) and differential thermal analysis (DTA).

Ternary Ag–Cu–Ni alloys with various compositions were prepared for phase equilibria study. Silver and copper shots and nickel wire of 99.99% purity were weighed to an accuracy of $\pm$ 0.001 g. By using an arc melter, the weighed nickel wire and copper shots were melted under an argon atmosphere first, and then the weighed silver shots were introduced and alloyed together. The alloy pellet was turned upside down during the alloying process in the arc-melter furnace several times to increase homogeneity.

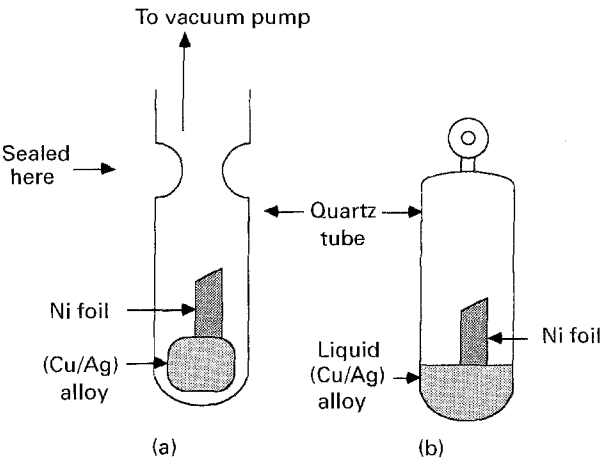

Figure 1 A schematic diagram of the reaction diffusion couple capsule, (a) before reaction, (b) after reaction.

2.2. Phase equilibria study

The Ag–Cu–Ni alloy pellet removed from the arc melter was sealed in a quartz tube under a 10^{-3} torr vacuum. The sample capsule was held in a furnace at a predetermined temperature for a predetermined reaction time. Phase equilibria were determined at three different temperatures: 700, 795 and 860 °C. The longest reaction time lasted 45 days for the samples annealed at 700 °C, and 200 h for the samples annealed at 795 and 860 °C. The sample capsule was then removed from the furnace and quenched into icy water. The sample was cut in half. One half was prepared for phase identification by using X-ray diffractometer (XRD), and the other half was mounted for metallurgical examination using optical microscopy (OM), scanning electron microscopy (SEM) and electron probe microanalysis (EPMA)–wavelength dispersive spectrometry (WDS).

2.3. Reaction diffusion couple study

Two different types of reaction diffusion couples were prepared: type I, Ag–28.0 wt % Cu alloy/pure nickel foil, and type II, Ag–15.0 wt % Cu alloy/pure nickel foil. 500 mg Ag–Cu alloy was cut from the quenched alloy ingot, and encapsulated in a vacuumed quartz tube with a piece of 3 mm × 15 mm × 1 mm nickel foil. The encapsulated capsules were held in furnaces at 795 and 860 °C for types I and II couples, respectively. These two temperatures were 15 °C higher than the melting points of the respective Ag–Cu alloys, and yet lower than the melting point of pure nickel foil. At these temperatures, the solid nickel foil was surrounded by and reacted with the molten Ag–Cu alloy. A schematic diagram of the preparation of the diffusion couple is shown in Fig. 1. For the purpose of comparison, type I reaction diffusion couples annealed at 860 and 700 °C were also investigated. At 700 °C, both nickel foil and Ag–28 wt % Cu alloy stayed in the solid state. The sample capsule of the solid/solid couple was first prepared by a similar practice to that mentioned above. The contact of the nickel and Ag–Cu alloys was formed by heating the encapsulated capsule to 795 °C for a very short period of time to melt the Ag–Cu alloy. Then the capsule was quenched into icy water, and annealed at 700 °C. The duration of the reaction time of the couples varied from 2 h to 6 days. At the end of the preset reaction time, the capsule was removed from the furnace and quenched into icy water.

The interface between the nickel foil and the Ag–Cu alloy of the reaction diffusion couple was first located. Then the couple was mounted and polished, so that the vertical section of the interface was exposed for metallurgical examination by using OM and SEM. Compositional analysis of the reaction layers was conducted by using EPMA (WDS).

3. Results and discussion

3.1. Experimental determination of phase equilibria

The nominal compositions of the Ag–Cu–Ni ternary alloys examined in this study are listed in Table I. Because high nickel-content alloys have very high melting points, and experimental difficulties would be encountered in determining their phase equilibria, the ternary alloys were all in the low nickel-content region as shown in Figs 2–4. A typical microstructure of the alloys, e.g. the Ag–50.0 wt % Cu–5.0 wt % Ni alloy, after being annealed at 860 °C is shown in Fig. 5. Prior to quenching, the dark phase was the solid phase, and the eutectic phase was the liquid phase. The compositions of the dark phase and the eutectic phase were examined by using EPMA, and the results are shown in Fig. 2 and Table I. Similar results were obtained for the alloys annealed at 795 °C, and the tie-line information was summarized in Fig. 3 and Table I. Only (Cu, Ni) and Ag phases, without any ternary compound, were observed from XRD and the metallurgical analysis. These results were in agreement with the data in the literature [19–21]. Different microstructure was noticed for the alloys annealed at 700 °C. As shown in Fig. 6 for the Ag–90.91 wt % Cu–1.05 wt % Ni alloy, the equilibrium phases were determined to be (Cu, Ni) phase the dark phase), and Ag phase (the bright phase).

TABLE I Phase equilibria of the Ag–Cu–Ni ternary alloys experimentally investigated in this study

Nominal composition (at %)	Annealing temperature (°C)	Composition of the copper–nickel phase (Cu, Ni)	Composition of the liquid phase(L) or the Ag-rich phase (Ag)
Ag–91.0Cu–1.0Ni	860	Ag–93.5 Cu–0.8 Ni(Cu,Ni)	Ag–36.2 Cu–0.1 Ni(L)
Ag–81.0 Cu–2.0 Ni	860	Ag–91.9 Cu–2.7 Ni(Cu,Ni)	Ag–40.8 Cu–0.2 Ni(L)
Ag–72.0 Cu–3.0 Ni	860	Ag–89.9 Cu–5.3 Ni(Cu,Ni)	Ag–38.2 Cu–0.1 Ni(L)
Ag–60.0 Cu–4.0 Ni	860	Ag–85.8 Cu–10.5 Ni(Cu,Ni)	Ag–36.8 Cu–0.1 Ni(L)
Ag–50.0 Cu–5.0 Ni	860	Ag–80.3 Cu–16.9 Ni(Cu,Ni)	Ag–38.1 Cu–0.2 Ni(L)
Ag–90.0 Cu–2.1 Ni	795	Ag–90.4 Cu–2.5 Ni(Cu,Ni)	Ag–36.1 Cu–0.1 Ni(L)
Ag–37.0 Cu–3.0 Ni	795	Ag–87.4 Cu–9.1 Ni(Cu,Ni)	Ag–10.0 Cu–0.4 Ni(Ag)
Ag–26.4 Cu–3.6 Ni	795	Ag–83.0 Cu–14.2 Ni(Cu,Ni)	Ag–9.9 Cu–0.5 Ni(Ag)
Ag–90.9 Cu–1.1 Ni	700	Ag–96.3 Cu–0.9 Ni(Cu,Ni)	Ag–12.9 Cu–0.4 Ni(Ag)
Ag–81.0 Cu–2.0 Ni	700	Ag–95.7 Cu–2.2 Ni(Cu,Ni)	Ag–14.6 Cu–0.5 Ni(Ag)
Ag–72.0 Cu–3.0 Ni	700	Ag–93.1 Cu–4.4 Ni(Cu,Ni)	Ag–10.8 Cu–0.4 Ni(Ag)
Ag–60.0 Cu–4.1 Ni	700	Ag–91.8 Cu–6.4 Ni(Cu,Ni)	Ag–9.4 Cu–0.4 Ni(Ag)
Ag–49.9 Cu–5.0 Ni	700	Ag–88.2 Cu–9.8 Ni(Cu,Ni)	Ag–9.1 Cu–0.7 Ni(Ag)
Ag–30.3 Cu–3.6 Ni	700	Ag–85.3 Cu–12.7 Ni(Cu,Ni)	Ag–6.9 Cu–0.3 Ni(Ag)
Ag–24.1 Cu–3.9 Ni	700	Ag–82.4 Cu–15.7 Ni(Cu,Ni)	Ag–5.5 Cu–0.3 Ni(Ag)

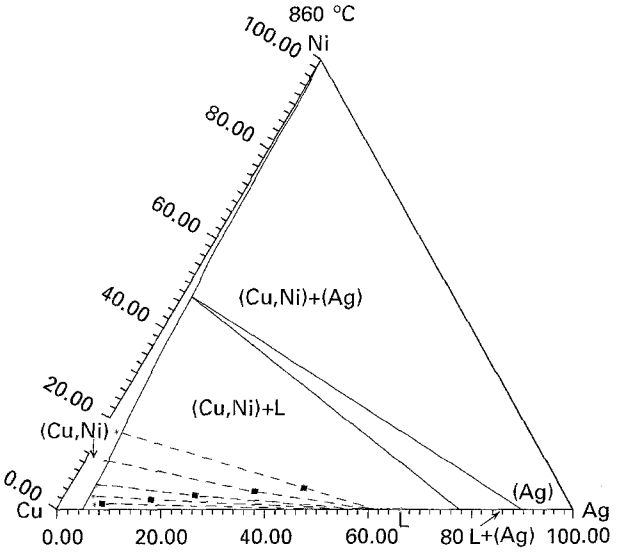

Figure 2 The experimentally determined tie lines superimposed with the calculated isothermal section at 860 °C. (■) Nominal composition, (*) composition of the equilibrium phase determined using EPMA.

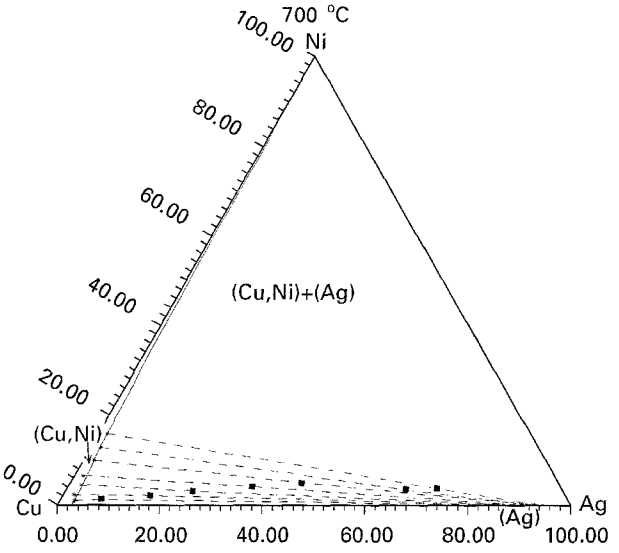

Figure 4 The experimentally determined tie lines superimposed with the calculated isothermal section at 700 °C. (■) Nominal composition, (*) composition of the equilibrium phase determined using EPMA.

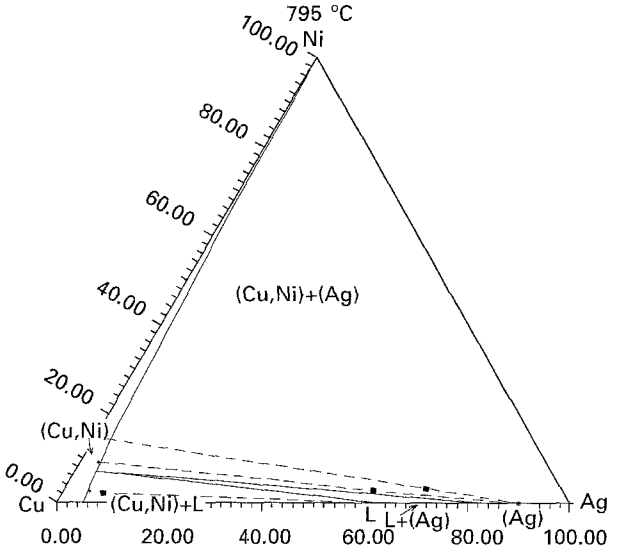

Figure 3 The experimentally determined tie lines superimposed with the calculated isothermal section at 795 °C. (■) Nominal composition, (*) composition of the equilibrium phase determined using EPMA.

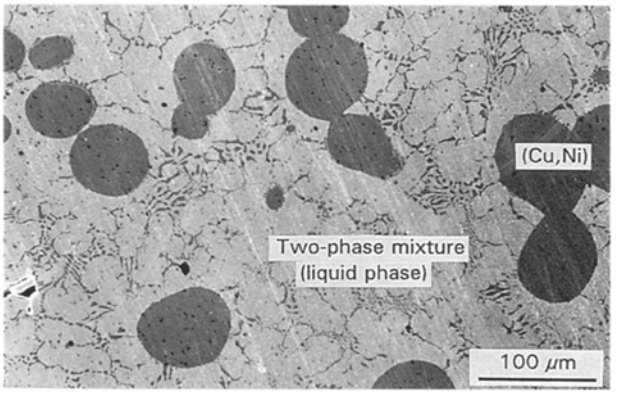

Figure 5 A scanning electron micrograph of the microstructure of the Ag–50 wt % Cu–5 wt % Ni alloy annealed at 860 °C for 200 h.

3.2. Phase diagram calculation

3.2.1. Binary systems

The three pertinent binary phase diagrams, Ag–Cu, Cu–Ni and Ni–Ag, have been calculated and are

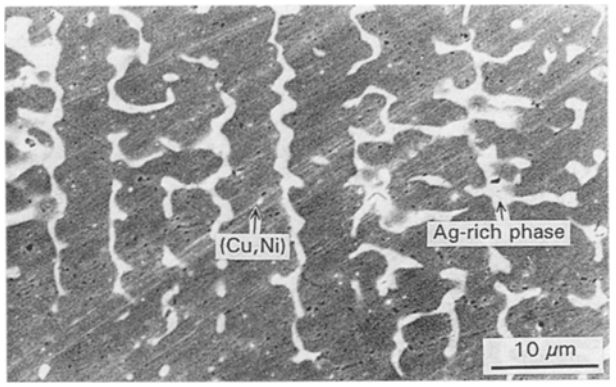

Figure 6 A scanning electron micrograph of the microstructure of the Ag–90.91 wt % Cu–1.05 wt % Ni alloy annealed at 700 °C for 45 days.

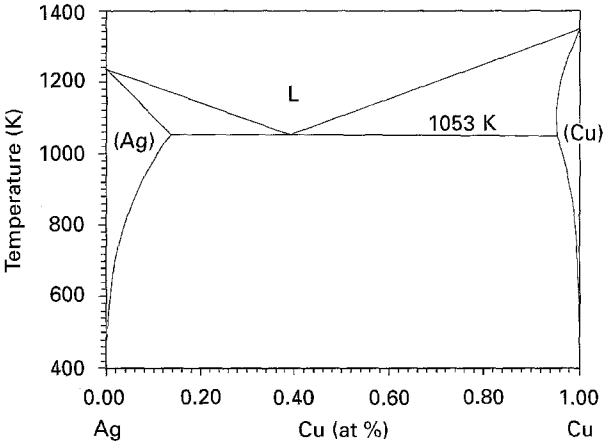

Figure 7 The calculated Ag–Cu phase diagram.

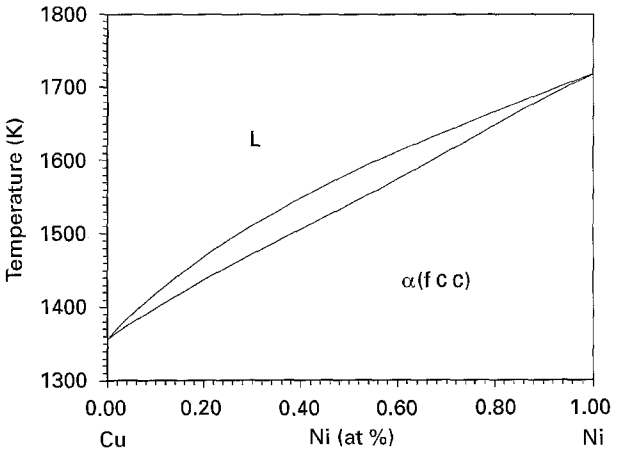

Figure 8 The calculated Cu–Ni phase diagram.

shown in Figs 7–9. The Ag–Cu is a simple eutectic system [22], with a miscibility gap between the f c c silver and the f c c copper solid solutions, and a completely mixed liquid phase. Its eutectic reaction, L → Ag(f c c) + Cu(f c c), occurs at 778 °C and Ag–28.0 wt % Cu. The Cu–Ni is an isomorphous system [23] at high temperatures, while the f c c phase exhibits a miscibility gap at the temperatures lower than 355 °C. The very limited studies [24–26] have shown that the Ni–Ag system has two invariant

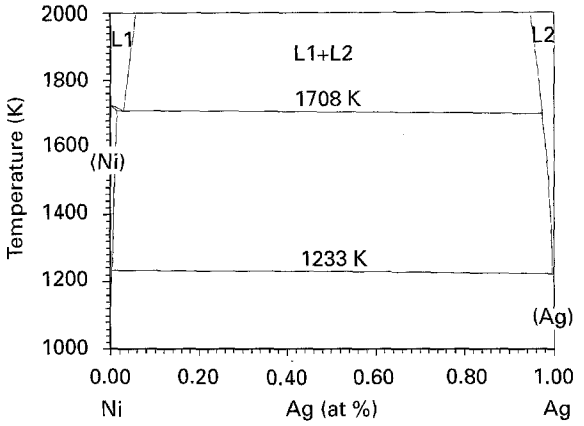

Figure 9 The calculated Ag–Ni phase diagram.

reactions: a eutectic reaction, L → Ni + Ag, at 960 °C, and a monotectic reaction $L_I \rightarrow L_{II}$ + Ni, at 1435 °C.

Owing to its relatively simplistic nature and also experimental interest in rapid solidification, the Ag–Cu system has been quite extensively studied. Complete thermodynamic evaluations of the Ag–Cu system have also been carried out by Murray [22], and recently by Subramanian and Perepezko [27]. These two evaluations gave very similar descriptions of the stable phase equilibria, and the results deviated mostly in the metastable phase equilibria. The thermodynamic assessment of the Ag–Cu system by Murray [22] has been adopted in this study. However, the values used in this study regarding the corresponding lattice stability of silver and copper are from Hultgren *et al.* [28] and are different from those given by Murray [22]. The excess Gibbs' energies of the liquid phase and the f c c phase are represented by the following equations

$$\frac{\Delta^{xs}G^{L}}{RT} = \tfrac{1}{2}\, x_i x_j \left[(w_{ij}^{L} + w_{ji}^{L}) + (w_{ij}^{L} - w_{ji}^{L})(x_j - x_i)\right] \quad (1a)$$

$$\frac{\Delta^{xs}G^{\alpha}}{RT} = \tfrac{1}{2}\, x_i x_j \left[(w_{ij}^{\alpha} + w_{ji}^{\alpha}) + (w_{ij}^{\alpha} - w_{ji}^{\alpha})(x_j - x_i)\right] \quad (1b)$$

where R is the gas constant and the values of the interaction parameters, w_{ji}^{L}, w_{ij}^{L} and w_{ji}^{α}, w_{ij}^{α}, are given in Table II.

The Cu–Ni system has been studied previously by one of the authors [23]. Only the high-temperature range is of interest in this study, while the possible miscibility gap at lower temperatures is not of concern. In the high-temperature range, i.e. higher than 600 °C, the magnetic effect can be ignored. The excess Gibbs' energies of the liquid and f c c phases are both described by Equation 1. The thermodynamic parameters used are listed in Table II.

Only very limited studies were conducted on the Ni–Ag system. The most recent phase equilibria assessment is by Singleton and Nash [24], and yet with no complete thermodynamic evaluations. The solution model was adopted in this study to describe the

TABLE II Thermodynamic parameters of the Ag–Cu–Ni system

Lattice stability	Solution parameters[a]		
$\Delta G_{Ni}^{fcc\to L} = -17472.0 + 10.12\,T$	$W_{12}^{L} = 6314.6/T$	$W_{12}^{\alpha} = 6795.8/T$	$W_{11}^{L} = 0$
$\Delta G_{Ag}^{fcc\to L} = -11945.0 + 9.67\,T$	$W_{21}^{L} = 6314.6/T$	$W_{21}^{\alpha} = 6795.8/T$	$W_{22}^{L} = 0$
$\Delta G_{Cu}^{fcc\to L} = -13054.0 + 9.623\,T$	$W_{23}^{L} = 2116.4/T - 0.41893$	$W_{23}^{\alpha} = 4874.7/T - 1.31140$	$W_{33}^{L} = 0$
	$W_{32}^{L} = 1553.1/T - 0.19136$	$W_{32}^{\alpha} = 3432.3/T - 0.89644$	$W_{11}^{\alpha} = 0$
	$W_{13}^{L} = 1292.8/T$	$W_{13}^{\alpha} = 300/T + 0.57658$	$W_{22}^{\alpha} = 0$
	$W_{31}^{L} = 1517.1/T$	$W_{31}^{\alpha} = 1400.0/T + 0.01667$	$W_{33}^{\alpha} = 0$

[a] 1, Ni; 2, Ag; 3, Cu; α, fcc; L, liquid.

thermodynamic behaviour of the nickel and liquid phases. The silver phase has been assumed to be pure element with no nickel solubility. Owing to the lack of experimentally determined thermodynamic data, the parameters in the models, as shown in Equation 1, have been obtained by the iterated calculation of the phase diagram. The parameters are shown in Table II.

3.2.2. Ternary systems

Chang *et al.* [29] assessed the Ag–Cu–Ni system in 1977 with two experimental determinations [19, 20] dated back to early this century. At about the same time, Siewart and Heine [21] studied the temperatures of the liquidus surface and the compositions of some tie lines. There is no ternary compound found in this system and the tie triangle of (Cu, Ni), Ag, and liquid phases shifts toward the nickel corner with increasing temperatures. The liquid and the (Cu, Ni) phases are described by the following ternary solution models

$$\frac{\Delta^{xs}G^{L}}{RT} = \frac{1}{2}\sum_{j=1}^{3}\sum_{i=1}^{3}[w_{ij}^{L} + (w_{ij}^{L} - w_{ji}^{L})x_j]\,x_j x_i \qquad (2a)$$

$$\frac{\Delta^{xs}G^{\alpha}}{RT} = \frac{1}{2}\sum_{j=1}^{3}\sum_{i=1}^{3}[w_{ij}^{\alpha} + (w_{ij}^{\alpha} - w_{ji}^{\alpha})x_j]\,x_j x_i \qquad (2b)$$

where w_{ji}^{L}, w_{ij}^{L} and w_{ji}^{α}, w_{ij}^{α} are binary parameters. In this study, an ideal mixing between these binary alloys is assumed for the liquid and (Cu, Ni) phases and no ternary interaction parameters are used. The silver phase is assumed to be a binary solution without nickel solubility. The calculated isothermal sections at 700, 795 and 860 °C are shown in Figs 2–4, respectively. The results are in agreement with the experimentally determined phase boundaries.

3.3. Reaction diffusion couple study

3.3.1. Liquid couples at 795 °C

As shown in Fig. 10, a reaction zone was developed for the type I liquid diffusion couple annealed at 795 °C for 6 h. It can be noticed that the interface was non-planar, and the reaction zone consisted of a two-phase mixture. The reaction zone had a larger amount of the bright phase on the liquid side, while the larger amount of the dark phase was on the nickel side. Quantitative analysis by using EPMA was carried out to determine the compositions of the phases from the nickel foil through the reaction layer to the liquid phase. It is indicated that a (Cu, Ni) layer was developed at the nickel reaction layer interface, and the bright phase was silver phase. The results were plotted on the 860 °C isothermal section as shown in Fig. 11. The determined diffusion path was Ni/(Cu, Ni)/Ag/liquid. This diffusion path was in agreement with the phase diagram calculation as shown in Fig. 11. Similar results were obtained for type I couples annealed at 795 °C for various periods of reaction time.

The growth rate of the reaction layer was determined by measuring the thickness of the reaction layer versus the annealing time. Because the interface was

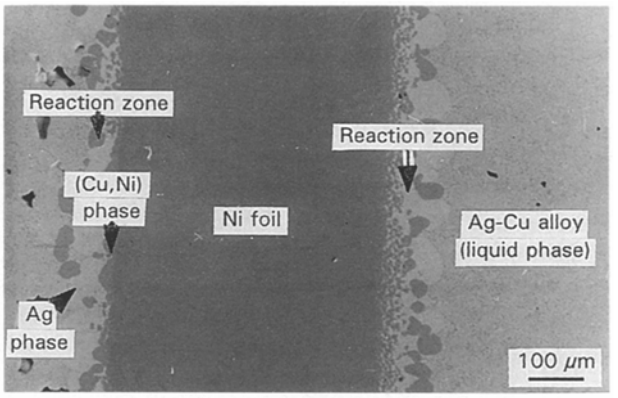

Figure 10 A scanning electron micrograph of the solid Ni/molten Ag–28 wt % Cu reaction diffusion couple annealed at 795 °C for 6 h.

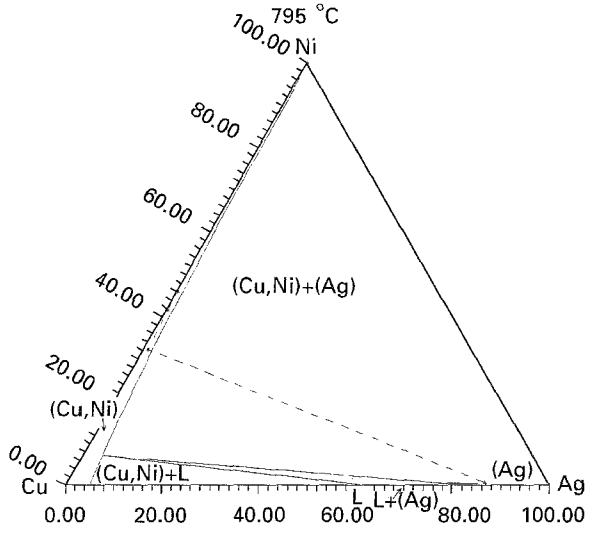

Figure 11 Diffusion path of the solid Ni/molten Ag–28 wt % Cu couple determined using an EPMA line scan superimposed with the calculated isothermal section at 795 °C. (---) Diffusion path, (*) composition determined using EPMA line scan.

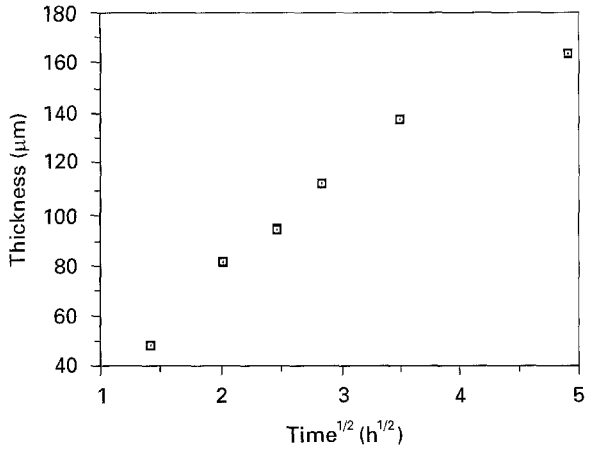

Figure 12 The growth rate of the reaction layer from the solid Ni/molten Ag–28 wt % Cu couples annealed at 795 °C. (□) Thickness of the reaction layer determined using image analyses.

not planar, the thickness was determined by measuring the area of the reaction layer divided by the linear distance of the interface by using an image analyser, i.e. an average thickness was reported. The results were ploted versus the square root of reaction time as shown in Fig. 12. It can be seen that the growth rate of the reaction layer followed the parabolic law, which indicated that the growth mechanism of the reaction layer was by bulk diffusion control.

3.3.2. Liquid couples at 860 °C

A very different morphology was observed for the type II diffusion couple annealed at 860 °C for 2 days as shown in Fig. 13a. Instead of a clear reaction layer as in the case of type I diffusion couple annealed at 795 °C, "cracking" was found along the nickel foil. The "cracks" penetrated into the nickel foil with increasing of reaction time. After 1 month, "cracks" were observed through the whole nickel foil as shown in Fig. 13b. Elemental X-ray mapping of nickel, copper and silver elements indicated that the cracks were filled with molten Ag–Cu alloy. Quantitative analysis by using EPMA was conducted from the centre of one "island" through the "river" (the crack) to the centre of another island, and the results were plotted in Fig. 14. It indicated that the possible phase formation sequence was similar to the type I couple annealed at 795 °C, and it was Ni/(Cu, Ni)/Ag/liquid. The results obtained from the two different types of liquid diffusion couples were in agreement with the phase equilibria study that there was no ternary compound and the tie triangle of (Cu, Ni), Ag, and liquid phases shifted towards the nickel corner as temperature increased.

In the liquid couples, two different mechanisms, dissolution and formation of solid phases, were competing. The growth of the reaction zone would be observed only if its growth rate was faster than the dissolution rate. It was speculated that for the type II couples annealed at 860 °C, the rate of dissolution was faster than that of the formation of the silver layer. Thus only a very thin layer of silver existed; even the determined diffusion path was the same as that of the

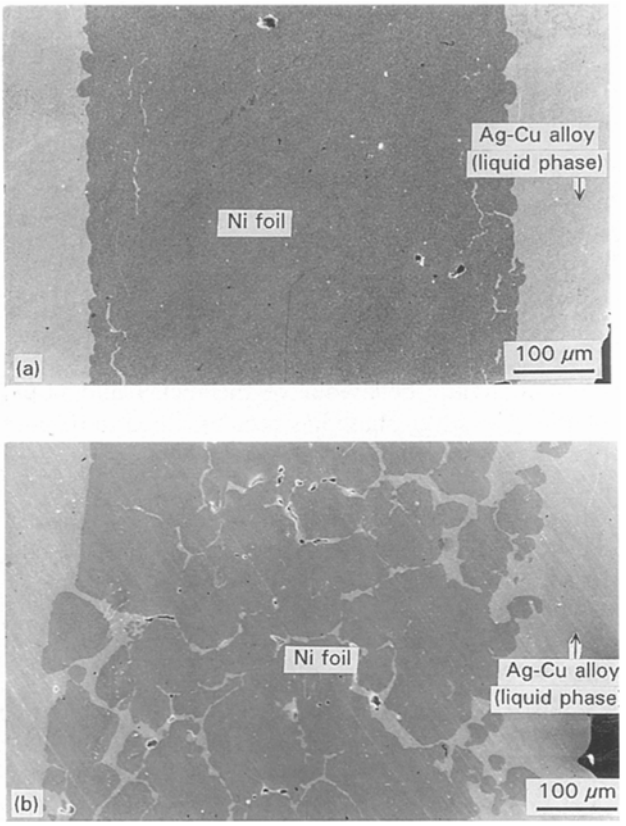

Figure 13 Scanning electron micrographs of (a) the solid Ni/molten Ag–15 wt % Cu diffusion couple annealed at 860 °C for 2 days, and (b) the solid Ni/molten Ag–15 wt % Cu diffusion couple annealed at 860 °C for 1 month.

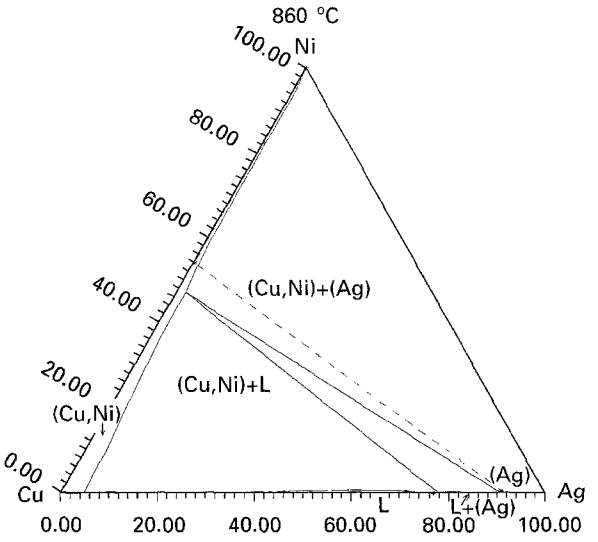

Figure 14 Diffusion path of the solid Ni/molten Ag–15 wt % Cu couple determined using an EPMA line scan superimposed with the calculated isothermal section at 860 °C for 2 days. (- - -) Diffusion path, (*) composition determined using EPMA line scan.

type I couples annealed at 795 °C. It was also speculated that the dissolution rate along the grain boundary was faster than the erosion of the bulk phase, so that the phenomenon of liquid penetration into the nickel foil would occur. Inside the "crack", the amount of liquid was less, the dissolution rate became slower, the growth of the solid reaction zone became

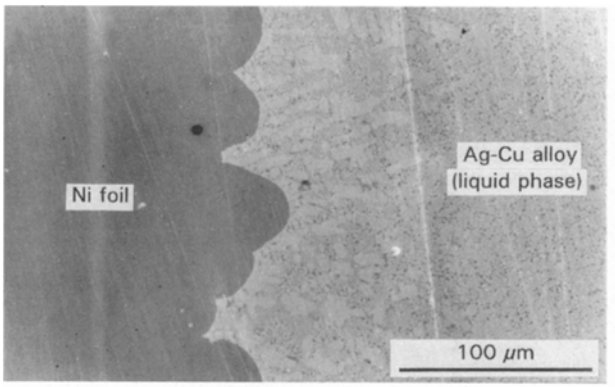

Figure 15 A scanning electron micrograph of the solid Ni/molten Ag–28 wt % Cu diffusion couple annealed at 860 °C for 4 days.

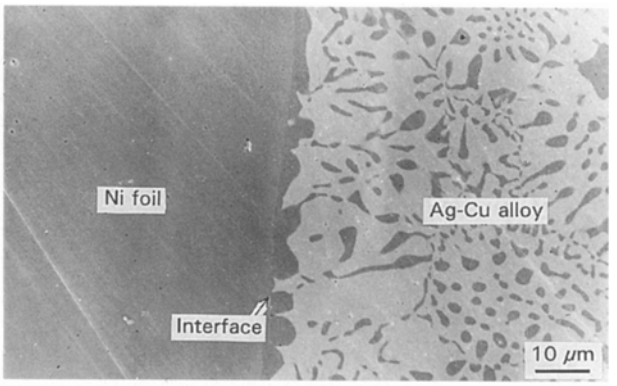

Figure 17 A scanning electron micrograph of the solid Ni/solid Ag–28 wt % Cu diffusion couple prior to annealing treatment.

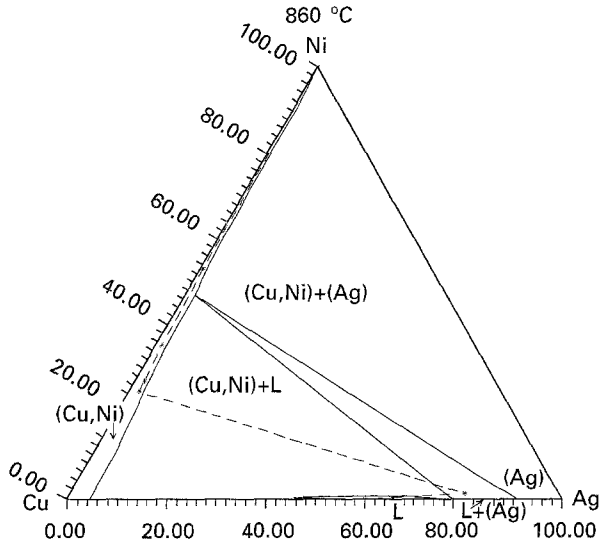

Figure 16 Diffusion path of the solid Ni/molten Ag–28 wt % Cu couple determined using an EPMA line scan superimposed with the calculated isothermal section at 860 °C for 4 days. (– – –) Diffusion path, (*) composition determined using EPMA line scan.

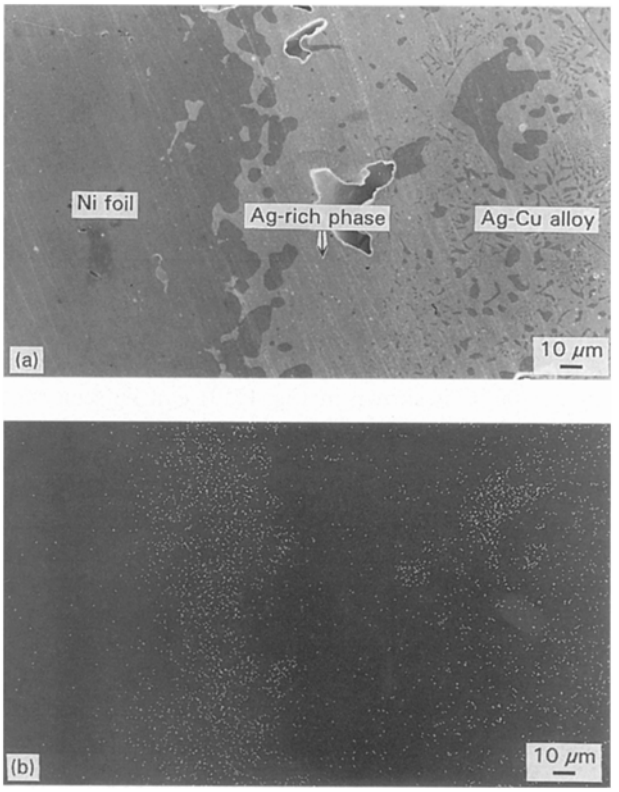

Figure 18 (a) A scanning electron micrograph of the solid Ni/solid Ag–28 wt % Cu diffusion couple annealed at 700 °C for 8 weeks. (b) Cu-elemental X-ray mapping of the solid Ni/solid Ag–28 wt % Cu diffusion couple annealed at 700 °C for 8 weeks.

more vivid, so that the diffusion path can be determined. However, further studies are still required to prove this theory.

Compared with the two previously mentioned liquid couples, a different diffusion path was found for the type I diffusion couples annealed at 860 °C. As shown in Fig. 15, the morphology was different from the two above-mentioned couples except that they all displayed non-planar interfaces. The formation of a thick reaction layer or cracks inside the nickel foil were not observed in this couple. The EPMA results were plotted with the calculated isothermal section, as shown in Fig. 16. Based on the results of metallographic and compositional analysis, the diffusion path was Ni/(Cu, Ni)/Ag-rich liquid/liquid. As can be seen in Fig. 16, the experimentally determined composition of the silver-rich liquid phase was in the tie-triangle region. Because the liquid phase became a two-phase mixture after quenching, the determination of the composition of the liquid phase had large uncertainties. If this experimental difficulty was taken into consideration, the phase equilibria study should be considered to be in agreement with the EPMA results and the diffusion path was as mentioned. Because the diffusion paths were different between the type I couples annealed at 795 °C and those at 860 °C, their interfacial morphologies differed accordingly. The (Cu, Ni) phase was in equilibrium with the liquid phase for the type I couple during annealing at 860 °C, and the thin silver layer was a result of solidification during quenching. Unlike the type I couples annealed at 795 °C, the (Cu, Ni) phase was in equilibrium with the solid silver phase, and the thick silver layer was formed as a result of the diffusion growth during annealing.

3.3.3. Diffusion couples at 700 °C

For the purpose of comparison, the interfacial reaction between solid nickel and solid Ag–28 wt % Cu

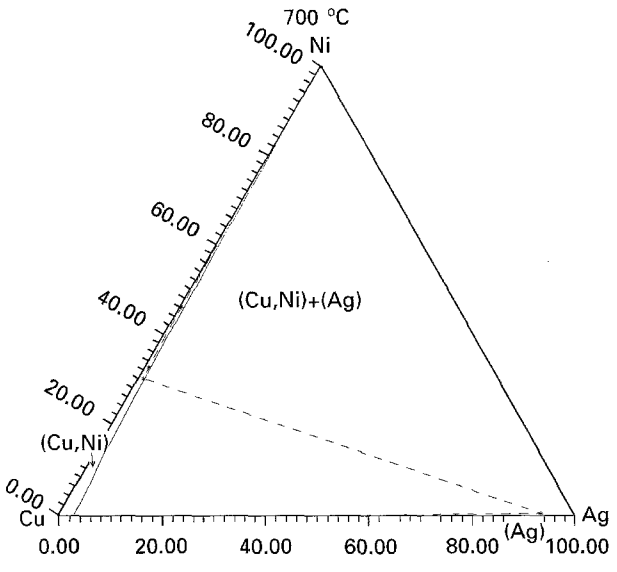

Figure 19 Diffusion path of the solid Ni/solid Ag–28 wt % Cu couple determined using an EPMA line scan superimposed with the calculated isothermal section at 700 °C for 8 weeks. (– – –) Diffusion path, (*) composition determined using EPMA line scan.

alloy were investigated in addition to those with molten Ag–Cu alloys. As mentioned previously, the couple was prepared by melting the Ag–Cu alloy and then quenched to make the contact. The morphology of the interface of the diffusion couple prior to annealing at 700 °C is shown in Fig. 17. It can be seen that the boundary between the solid nickel foil and liquid was still very clear, and it can also be noticed that during solidification the nickel phase tended to nucleate and grow on the nickel foil. After annealing at 700 °C for 8 weeks, a non-planar interface was developed and it can also be noticed that the silver layer grew, as shown in Fig. 18a. The existence of the silver and also the (Cu, Ni) layers can be observed by using the copper elemental X-ray mapping as shown in Fig. 18b. However, a clear boundary between the silver phase and the eutetic phase could not be drawn easily. Quantitative analysis results obtained by using EPMA were superimposed with the calculated isothermal section as shown in Fig. 19. The diffusion path determined was in agreement with the calculated phase relationship, and was Ni/(Cu, Ni)/Ag/(eutectic).

4. Conclusion

Isothermal sections of the Ag–Cu–Ni system at 700, 795 and 860 °C were determined by both experimental determination and model calculation. One liquid phase and two solid phases, the (Cu, Ni) phase and the silver phase existed at these temperatures, and no ternary compound was found. These isothermal sections also demonstrated that the tie triangle shifted towards the nickel side as temperature increased. This phase equilibria information was used with the diffusion couple studies to investigate the phases formed at the interfaces between solid nickel and Ag–Cu alloys. The phase sequences at the interfaces of the couples were Ni/(Cu, Ni)/Ag/liquid, Ni/(Cu, Ni)/Ag/liquid, Ni/(Cu, Ni)/liquid, Ni/(Cu, Ni)/Ag/eutectic, for the solid Ni/molten Ag–28 wt % Cu alloy (type I) couple annealed at 795 °C, solid Ni/molten Ag–15 wt % Cu alloy (type II) couple annealed at 860 °C, type I couple annealed at 860 °C, and type I couple annealed at 700 °C, respectively. The morphologies of the interfaces were all non-planar and all differed between the four diffusion couples investigated. Type I couples annealed at 795 °C had a thick reaction zone. Penetration of "cracks" into the nickel foil was found for type II at 860 °C. A clear reaction zone was not found for the type I couples annealed at 860 °C, and a (Cu, Ni) layer could only be seen by using elemental X-ray mapping. The different morphologies resulted from various factors, such as the different diffusion paths and different dissolution rates. Further studies are important and will stimulate detailed exploration of the growth mechanism of liquid couples. The growth rate of the reaction zone for the type I couple at 795 °C was determined and a parabolic law was followed, which indicated that the growth mechanism was by bulk diffusion control.

Acknowledgement

This study was funded by the National Science Council in Taiwan, through Grant NSC82-0405-E-007-285. The authors thank Ms A.-H. Liu and Ms S.-Y. Tsai for carrying out the SEM and EPMA experiments.

References

1. D. P. SERAPHIM, R. C. LASKY and C.-Y. LI, "Principles of Electronic Packaging" (McGraw-Hill, New York, 1989).
2. Y. HAMANO and M. TERASAWA, in "Materials Research Society Symposia Proceedings", Vol. 72, "Electronic Packaging Materials Science II", edited by K. A. Jackson, R. C. Pohanka, D. R. Uhlmann and D. R. Ulrich (MRS, Pittsburgh, PA, 1986) pp. 3–12.
3. D. A. WEIRAUCH Jr, *Weld. Res. Suppl.* (1994) 110s.
4. S. C. DEV, P. BASAK, I. SINGH, R. K. DUBEY and O. N. MOHANTY, *J. Mater. Sci.* **27** (1992) 6646.
5. S.-W. CHEN, *Mater. Chem. Phys.* **33** (1993) 271.
6. C. WAGNER, *J. Electrochem. Soc.* **103** (1956) 571.
7. J. E. LANE and J. S. KIRKALDY, *Can. J. Phys.* **42** (1964) 1643.
8. M. M. P. JANSSEN and G. D. RIECK, *Trans. TMS-AIME* **239** (1967) 1372.
9. R. A. RAPP, A. FZIS and G. J. YUREK, *Metall. Trans.* **4** (1973) 1283.
10. F. J. J. VAN LOO, J. A. VAN BEEK, G. F. BASTIN and R. METSELAAR, in "Diffusion in solids: Recent developments", edited by M. A. Dayanada and G. E. Murch (TMS, Warrendale, PA, 1984) pp. 231–59.
11. J.-C. LIN, K. J. SCHULZ, K.-C. HSIEH and Y. A. CHANG, *J. Electrochem. Soc.* **136** (1989) 3006.
12. C. R. KAO and Y. A. CHANG, *Acta. Metall. Mater.* **41** (1993) 3463.
13. A. G. WARD and J. W. TAYLOR, *J. Metals* **85** (1956) 145.
14. J. M. LOMMEL and B. CHALMERS, *Trans. TMS-AIME* **215** (1959) 499.
15. S. K. KANG and V. RAMACHANDRAN, *Scripta Metall.* **14** (1980) 421.
16. H. NAKAGAWA, C. H. LEE and T. H. NORTH, *Metall. Trans.* **22A** (1991) 543.
17. Y. WANG, H. K. KIM, H. K. LIOU and K. N. TU, *Scripta Metall. Mater.* (1995) accepted.
18. C.-L. TSAO and S.-W. CHEN, *J. Mater. Sci.* **30** (1995) 5215.
19. P. DE CESARIS, *Gazz. Chim. Ital.* **43** (1913) 365.

20. W. GUERTLER and A. BERGMANN, *Z. Metallkde* **25** (1933) 53.
21. T. A. SIEWERT and R. W. HEINE, *Metall. Trans.* **8A** (1977) 515.
22. J. L. MURRAY, *Metall. Trans.* **15A** (1984) 261.
23. D. J. CHAKRABARTI, D. E. LAUGHLIN, S.-W. CHEN, and Y. A. CHANG, in "Binary Alloy Phase Diagrams", 2nd Edn, Vol. 2, edited by T. B. Massalski, H. Okamoto, P. R. Subramanian, and Kacprzak (ASM, Materials Park, OH 1990) pp. 1442.
24. M. SINGLETON and P. NASH, *Bull. Alloy Phase Diag.* **8** (1987) 119.
25. D. A. STEVENSON and J. WULFF, *Trans. Metall. AIME* **221** (1961) 271.
26. S. I. POPEL and V. N. KOZHURKOV, *Izv. Akad. Nauk. SSSR Metal* **2** (1974) 49.
27. P. R. SUBRAMANIAN and J. H. PEREPEZKO, *J. Phase Equilib.* **14** (1993) 62.
28. R. HULTGREN, P. D. DESAI, D. T. HAWKINS, M. GLEISER, K. K. KELLEY and D. D. WAGMAN, "Selected Values of the Thermodynamic Properties of the Elements" (ASM, Metals Park, OH, 1973).
29. Y. A. CHANG, D. GOLDBERG and J. P. NEUMANN, *J. Phys. Chem. Ref. Data* **6** (1977) 621.

Received 20 October 1995
and accepted 24 April 1996